Landscape Ecology **00:** 1–11, 2004.

Research article

A Simple Method for Estimating Potential Relative Radiation (PRR) for Landscape-Scale Vegetation Analysis

Kenneth B. Pierce Jr.*, Todd Lookingbill and Dean Urban
Nicholas School of the Environment and Earth Sciences, Duke University, Durham, NC 27708 USA;
**Author for correspondence (Tel.: 541 750-7393; Fax: 541 750-7329; E-mail: kpierce@fs.fed.us)*

Received ; accepted in revised form

Key words: Aspect, DEM, GIS, Solar insolation, Species-environment interactions, Topographic effects,Vvegetation distribution

Abstract

Radiation is one of the primary influences on vegetation composition and spatial pattern. Topographic orientation is often used as a proxy for relative radiation load due to its effects on evaporative demand and local temperature. Common methods for incorporating this information (i.e., site measures of slope and aspect) fail to include daily or annual changes in solar orientation and shading effects from local topography. As a result, these static measures do not incorporate the level of spatial and temporal heterogeneity required to examine vegetation patterns at the landscape level. We developed a widely applicable method for estimating potential relative radiation (PRR) using digital elevation data and a widely used geographic information system (Arc/Info). We found significant differences among four increasingly comprehensive radiation proxies. Our GIS-based proxy compared well with estimates from more data-intensive and computationally rigorous radiation models. We note that several recent studies have not found strong correlations between vegetation pattern and landscape-scale differences in radiation. We suggest that these findings may be due to the use of proxies that were not accurately capturing variability in radiation, and we recommend PRR or similar measures for use in future vegetation analyses.

Introduction

Plants respond to solar radiation through multiple pathways (Geiger 1965). Photosynthetically active radiation (PAR) provides the driving energy for photosynthesis (Raven et al. 1992). Radiation affects the water demand components of the water balance (Stephenson 1998), and has been shown to have a significant effect on the distribution of surface water through simulation modeling (Band et al. 1991) and empirical sampling (Yeakley et al. 1998). These multiple influences can result in complex responses to radiation loads. Numerous studies have shown that an interaction between radiation and plant processes can influence the landscape-scale distribution of plants (Swanson et al. 1988; Austin et al. 1990; Davis and Goetz 1990; Chen et al. 1999; Urban et al. 2000), but others, somewhat surprisingly, have not been able to document a strong correlation between radiation estimates and plant pattern (Brown 1994; Parker 1995; Park 2001).

Direct measurements of radiation are uncommon and especially rare in topographically rugged terrain. Acquiring fine-scale information about climatic factors over large extents is logistically problematic. There are two common approaches to account for radiation effects over landscape scales. The simpler approach relies on static topographic proxies based on slope and aspect, either from field measurements or from digital terrain data (e.g., Beers et al. 1966). A more complicated approach involves numerical integration of radiation values through simulation modeling using terrain and climate data (Running et al. 1987; Daly et al. 1994; Dubayah 1994; Dubayah and

XML — ms-code land03-269r2 — PIPS DO00001296 — 9 Aug 2004 — Grafikon 203066036

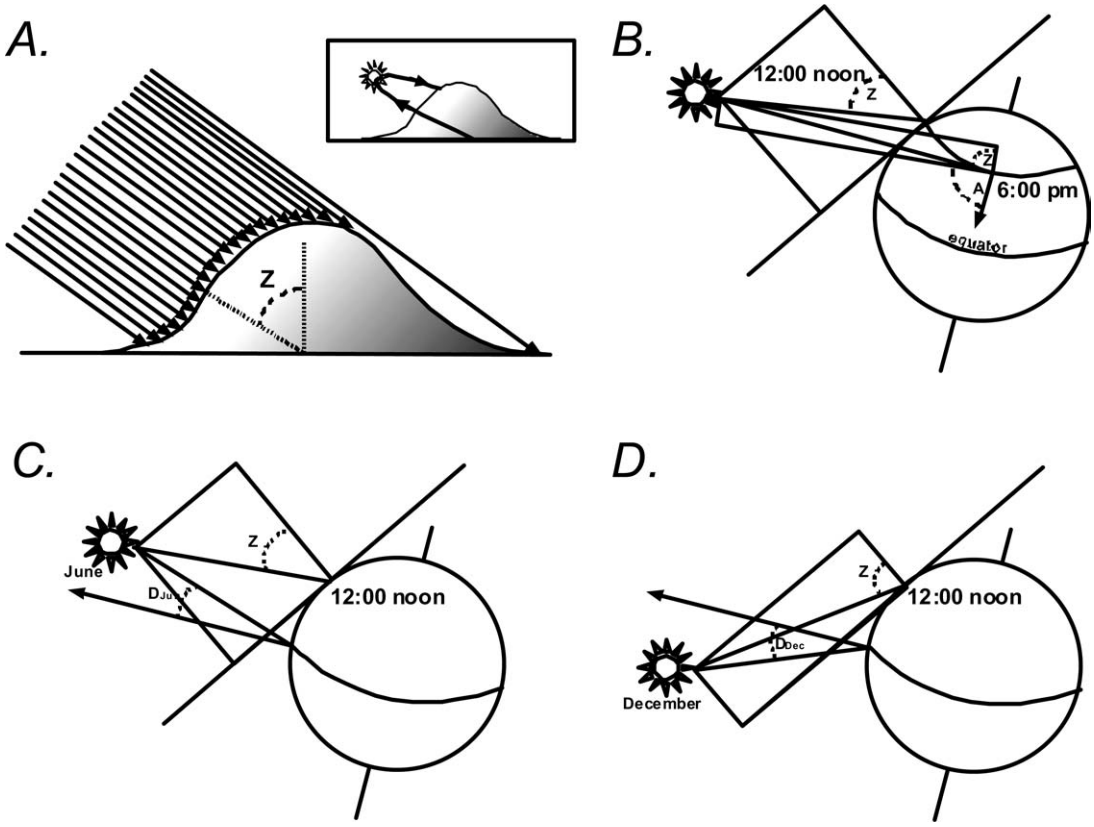

Figure 1. (A) Solar azimuth (*A*) and solar zenith angle (*Z*) create a topographic shading effect. (B) This shading is continuously shifting as the earth rotates causing changes in solar zenith and azimuth throughout the day. The change in the orientation of the earth's tilt in relation to the sun creates the basis for our seasons. The lower two panels depict the solar zenith (*Z*) and declination (*D*) for the same location during the summer (C.) and winter (D.) solstices.

Rich 1995; Thornton et al. 1997; Fu and Rich 1999; Wilson and Gallant 2000).

Here we present a third alternative: a physical proxy that captures some of the solar geometry of more complicated radiation models yet can be quickly implemented for any landscape with digital terrain data. This level of detail should be appropriate for landscape-scale vegetation analysis and provide a valuable addition to the spatial datasets available for ecological studies.

The geometry of radiation

Solar insolation is the sum of direct, diffuse and reflected radiation. Direct-beam radiation is the fraction of extra-atmospheric solar radiation that reaches the earth's surface without being scattered by molecules in the atmosphere (Figure 1a). Diffuse-beam radiation is the component resulting from atmospheric scattering. Reflected radiation is the component that bounces off other surfaces before impinging on a target (Campbell and Norman 1999). Under clear sky conditions, direct radiation is largely a function of the angle between the earth surface and the sun. Topography filters radiation loads through shading and attenuation of the solar flux by altering the solar illumination angle. The earth's rotation causes solar orientation to systematically change throughout the day (Figure 1a–b). The tilt and orbit of the earth causes solar orientation and solar period (Figure 1c–d) to systematically change throughout the year (Dubayah and Rich 1995). Simple radiation proxies can not account for these dynamics.

Diffuse and reflected radiation are more difficult to quantify (Dubayah and Rich 1995), and are not calculated in this method. These components tend to minimize spatial differences in radiation. Under clear sky conditions, the largest share of radiation is direct-beam. This condition provides the maximum contrast in radiation load between sites with different topo-

graphic orientations. As the partitioning of radiation shifts from direct to diffuse, sites are affected similarly and the relative differences between sites are reduced. Calculating a measure of potential direct radiation thus provides an upper bound on differences in solar insolation for topographically complex terrain.

Radiation proxies

Slope and aspect have been used as radiation proxies in hundreds of studies because, until recently, they have been the easiest way to estimate relative radiation. Early gradient analysis studies categorized topographic aspects as factors along a moisture continuum (e.g., Whittaker 1956). Frank and Lee (1966) standardized these discrete relationships between relative radiation and slope and aspect in tables that accounted for latitudinal differences. These tables were based on a 16-quadrant measure of aspect and are still in use today (Parker 1995; McCay et al. 1997; Donnegan and Rebertus 1999). As categorical factors, however, slope and aspect have a limited ability to capture the full range of topographic variability. For example, the 16-quadrant model has been used in several studies in the southern Appalachians with varying results (Day and Monk 1974; Clinton et al. 1994; McCay et al. 1997; Bolstad et al. 1998).

Aspect can be represented as a continuous quantity by reorienting the variable along a specified orientation of interest, such as a north-south axis. One common approach is to use 'absolute aspect' computed as ABS(180-aspect), which solves the circularity problem while aligning the index on a N-S axis. Beers et al. (1966) used the cosine function to transform aspect along an axis running from NE to SW to reflect the combined influence of bright illumination with warm afternoon temperatures maximally affecting SW-facing slopes of the Northern hemisphere. This transformation indexes radiation explicitly as a proxy for heat load or evaporative demand.

Radiation levels vary through time in several ways that are not captured by simple topographic proxies. For instance, east-facing slopes experience higher radiation loads in morning hours and decreased radiation in later afternoon hours. Annually, solar period changes in accordance with changing solar inclination. Therefore, incorporation of daily and annual solar path is essential when comparing solar exposure between two sites.

Even with proper consideration, slope and aspect alone might not be able to resolve radiation differences between sites. The proxies by necessity imply that observed slopes are in a landscape devoid of other features (*i.e.,* isolated mountains or hills). But obstructions to direct-beam radiation can result from not only 'self-shading' by the slope itself, but also from shading by nearby ridges. Two sites with identical topographic orientation (slope, aspect and elevation) can have widely differing solar exposure based on their topographic context. For example, sites could differ by being at the bottom of a drainage or the top of a nearby ridge but be characterized similarly by simple measures of slope and aspect. Radiation proxies, as well as non-spatial radiation models, do not incorporate shading effects from adjacent land features.

Radiation models

Quantitative estimations of radiation include the sum of the direct, diffuse and reflected components. Direct-beam radiation (R_b) to a spot on the horizontal plane of the earth can be estimated as(1)

where extra-atmospheric radiation (R_{ea}) is attenuated by atmospheric transmittance (t) and the cosine of the solar zenith angle (Z) which is the angle between a vector directed at the sun and one normal to the horizontal surface of the earth (Dubayah 1994). Transmittance is largely a function of the optical depth of the atmosphere and air pressure. The solar zenith angle is:

$$\cos(Z) = \sin(L) * \sin(D) + \cos(L) * \cos(D) * \cos(15(T - 12)) \quad (2)$$

where L is latitude, T is the time of day in hours, and the coefficient 15 represents the degrees of longitude the earth rotates each hour. Solar declination (D), the angle between the sun and a position directly above the equator at noon, accounts for the tilt of the earth. It depends only on time (Julian day J) and can be estimated for each day of the year as:

$$\sin(D) = 0.3978\sin[279.0 + 0.9856J + 1.9165\sin(356.6 + 0.9856J)] \quad (3)$$

The radiation calculations as described above are for

a flat plain on the earth's surface. Radiation is modified by local topography using tilt factors and view angles. Direct beam radiation is attenuated by tilt factors based on the solar azimuth (A) and local topography. The solar azimuth, the angle between a vector directed towards the equator and the vector directed towards the sun's current position in horizontal coordinates is calculated by

$$A = \arcsin\left[\left(\cos(D) * \sin\left(15(T-12)\right)/\cos(90-Z)\right)\right] \quad (4)$$

The solar azimuth (A), local slope (s) and local azimuth (a) are incorporated into the Hillshade function described in the methods section.

Diffuse-beam radiation is the fraction of radiation scattered by air molecules and aerosols that is not reflected back into space. The diffuse component is modified by taking into account the proportion of the sky visible from the point of estimation (i.e., the angular percentage of the hemispherical view). This is a small fraction in a deep chasm and close to 1.0 on a large flat plain. Sophisticated topographic radiation models like Solar Analyst (Fu and Rich 1999) or SRAD (Wilson and Gallant 2000) can account for this, though the viewshed calculation can take considerable time with large grids (McKenney et al. 1999). Reflected radiation is the sum of the direct and diffuse components multiplied by the local surface reflectivity of different surfaces [see Campbell and Norman 1998 for a more detailed accounting of these components]. The total radiation impinging on a surface is the sum of these three components.

Scientists have used these calculations to develop models for predicting solar radiation in complex terrain (Bonan 1988; Dozier and Frew 1990; Nikolov and Zeller 1992; Dubayah and Rich 1995; Greenland 1996; Wilson and Gallant 2000). Running these models can require considerable site data or the acquisition of special programs. For instance, SRAD requires up to 16 parameters to calculate a radiation map, however, literature values are often used in the absence of site data. (McKenney et al. 1999; Wilson and Gallant 2000). Our method uses the popular geographic information system Arc/Info (ESRI 1994) to produce a spatially explicit representation of variation in radiation with minimal investment in time or resources.

Summary

Our goal in calculating a new radiation proxy was to develop a dimensionless index to support community vegetation analysis. Decades of gradient studies have found vegetation patterns are primarily controlled by 'elevation' gradients with fine-scale topography and soils affecting patterns within the elevation gradient (Whittaker 1960; Dyrness et al. 1974; Kessell 1979; Austin et al. 1990). We were interested in the way local topography influences relative radiation load and thus evaporative demand. Previous studies suggest that this is an important mechanism controlling vegetation distributions (Callaway et al. 1998; Franklin et al. 2000; Mackey et al. 2000). For these applied uses, we felt a simple method of estimating relative radiation was needed that incorporated the important components of more complicated models but the ease of calculation of simple proxies. We show that current radiation proxies are insufficient for estimating the effect of insolation on hillslopes and should be replaced with a more explicit radiation estimate using either our method or a more complex radiation model.

Methods

Study sites

We demonstrate our approach for two study sites of complex topography in the western United States: the Kaweah Basin of Sequoia National Park, California and the H.J. Andrews Experimental Forest, Oregon.

Sequoia National Park is located on the west slope of the Sierra Nevada Mountains in southern California. We focus our study on a 7500 ha portion of the Kaweah Basin. Climate is Mediterranean with more than 90 percent of the annual precipitation falling from October through May (Stephenson 1998). The elevation in the Park ranges from 400 m to 4419 m (Vankat and Major 1978). The average slope on our plots was 18 degrees. Major vegetation types follow an elevation gradient from chaparral, through oak savannah, mixed conifer, and subalpine fir before reaching exposed granitic rock above treeline (Urban et al. 2000; Vankat and Major 1978). The Park's research emphasis includes the effects of climate on vegetation (Stephenson and Parsons 1993). As part of this research, we have gathered digital and field data and developed a forest simulation model, Facet, with a well-tested climate subroutine that will be used for

comparative purposes in this analysis (Miller and Urban 1999; Urban et al. 2000).

The H.J. Andrews Experimental Forest (HJA) is a Long Term Ecological Research (LTER) site located on the west slope of the Cascade Mountains. The Lookout Creek watershed covers 6400 ha and ranges in elevation from 410 m to 1630 m. Climate is characteristic of the Pacific Northwest, with dry summers and wet winters. Annual precipitation ranges from 2200 mm at the base station to 3400 mm at upper elevations, with less than 300 mm normally falling during the summer growing season (Grier and Logan 1977). Major vegetation types range from Douglas-fir/western hemlock at lower elevations, to Pacific silver fir and mountain hemlock at upper elevations (Franklin and Dyrness 1988). Like Sequoia NP, one of the major research emphases at HJA is the influence of climate on vegetation. Although radiation has been described as an important control on the distribution of several of the dominant tree species in the Western Cascades (*e.g.*, *Abies procera*), extending these relationships to large spatial scales has been problematic. A recent, detailed analysis of meteorological station data at the HJA provides a dataset for us to compare against the estimates of radiation derived from our simpler approach (Smith 2002).

Potential relative radiation (PRR)

To account for temporal variability in radiation, we developed potential relative radiation (PRR) as an integrative index, which sums hourly estimates of clear-sky radiation over the day and then sums daily values over the growing season. Each point estimate accounts for topographic shading by surrounding landscape features. The method can be summarized as follows.

1. Calculate solar inclination angle (the complement of solar zenith) and solar azimuth in degrees for daylight hours for the day of the month representing the average solar period for each month of the growing season (Equations 2 and 4; these data are also available on many websites).
2. Obtain a digital elevation model (DEM) of the study site (e.g., from USGS).
3. Calculate hourly hillshaded radiation grids using the DEM, solar azimuth and solar inclination (Arc/Info Hillshade function with Model Shadows option).
4. Sum hourly values to get daily totals, which represent monthly averages.
5. Sum monthly averages to get seasonal maps of PRR.

The approach is outlined in greater detail below.

There are many sources for finding solar azimuth and inclination for a specific location and time of day. Because solar path changes in a continuous manner throughout the year we used a single day from each month to represent that period (Klein 1977; Bonan 1988). We chose the day of the month that was closest to the average solar period for that month. This was not always the 15th of the month, but depended on the trajectory of the solar period for the month (*e.g.*, June 11 represents the average solar period for June).

We obtained a digital elevation model (DEM) for our study site from the USGS, being careful to incorporate enough surrounding area to properly capture topographic shading. We imported the DEM into Arc/Info and used solar position information with the Hillshade function,

$$HS = 255\left[\cos(90 - Z)\sin(s)\cos(\alpha - A) + \sin(90 - Z)\cos(s)\right] \quad (5)$$

where Z is the solar zenith, s is the local slope, A is the solar azimuth and α is the azimuth of the slope facet (ESRI 1994). Note that the Hillshade function uses solar inclination angle, which is the complement of solar zenith (90-Z).

This function calculates relative insolation based on surface orientation, solar position, and self-shading by calculating the angle between the vector normal to the plane of ground and solar position (ESRI 1994). We used the Model Shadows option to set areas shaded by surrounding topographic features to zero illumination. We performed this operation for each hour of daylight on the representative day of each month of the growing season. To calculate monthly radiation maps we summed over the hourly grids. To calculate relative seasonal radiation maps we summed the monthly grids.

Other radiation proxies

To compare the variation captured by our method to other common indices, we calculated three other radiation proxies. Two were derived both from field measurements and from DEM-based calculations. The first proxy was a simple measure of transformed

aspect (Urban et al. 2000) similar to Beers et al.'s (1966) measure but varying from −1 for NE facing slopes to 1 for southwest facing slopes:

$$TA = -1 * \cos(\alpha - 45) \quad (6)$$

The second proxy incorporated slope information by multiplying TA by the sine of the slope angle, so that steeper slopes are weighted accordingly:

$$TASL = -1 * \cos(\alpha - 45) * \sin(s) \quad (7)$$

We analyzed both DEM and field-based indices for these proxies to determine how well the digital data corresponded to on-the-ground measurements. We had field measurements of slope and aspect from 99 (20×20 m) plots in Kaweah Basin and 175 (20×20 m) plots in the HJA. We compared these field estimates to the DEM-based proxies for these same sets of plots.

The third radiation proxy we considered was a single Hillshade map. This proxy accounted for the effect of topographic shading without considering solar track. Hillshade requires the user to supply an azimuth and solar inclination angle (Equation 5). We used a solar azimuth of 225 degrees and solar inclination of 45 degrees to mirror our TA calculation.

Because we are interested in radiation as a relative variable in community ecology studies, not as an absolute variable in an atmospheric model, we did not correct insolation for atmospheric transmittance. We also ignored the effect of cloudiness. For landscape-scale vegetation analyses dealing with small-to-medium sized watersheds in mountainous regions, relative radiation estimates should be sufficient. We attempted to ascertain the effect of the simplifying assumptions in our method by comparing the results to those from two more complex radiation models individually parameterized for each site.

For Kaweah Basin, we used the radiation model from the forest gap simulator Facet (Urban et al. 2000). The simulator, derived from a general model by Bonan (1988) and Nikolov and Zeller (1992), has been shown to be generally robust at reproducing monthly empirical radiation values across North America on a variety of topographic positions (Urban et al. 2000). Because Facet simulates a single slope face, we ran individual simulations using data representative of the 99 points for which we had field measurements. We summed monthly values over the growing season (March through September) and compared the values to those calculated from the different proxies. Facet does not account for topographic shading.

For HJA, we compared our results to those from a model of radiation recently completed for the watershed that synthesizes the LTER meteorological data using PRISM (Parameter-elevation Regressions on Independent Slopes Model: Daly et al. 1994). These mean monthly estimates of radiation account for topography, cloudiness and their effects on direct and diffuse radiation (Smith 2002). We again summed monthly values over the growing season (June through September).

Results

A pronounced topographic feature from one of our study sites illustrates the differences among the different proxies. Figure 2 depicts the area around Moro Rock, a large granite dome in southern Sequoia National Park. The digital elevation map (Figure 2b) is provided for reference to the four proxies (Figure 2c–f). The transformed aspect image (Figure 2c) illustrates the difficulty of not including a measure of local slope in formulating a proxy. The dark streak across the center of the Figure is the northeast face of Moro Rock. The equally dark region in the upper right is a low-relief valley that also has a slight northeast aspect. When slope is accounted for (Figure 2d), the dark streak in the upper right becomes a lighter shade of gray, giving a much better representation of the contrast in topographic orientation.

The region depicted in Figure 2 lies in a region of the Park where the only major shading feature is Moro Rock. When topographic shading is considered (Figure 2e), the area of low light on the northeast side of Moro Rock is widened. No other shading effects are observed. The biggest change in the picture occurs when daily solar track is included (Figure 2f). The darkness in the upper right corner disappears and the darkness in the lower center becomes considerably lighter. This occurs because in the morning hours the sun is shining directly on some of these eastern-facing features for several hours. Morning sun is not captured by the other simple aspect proxies, which are transformed along a NE-SW axis. By integrating across the entire day, the PRR index also highlights features that get continuous full sun with distinctive radiation signatures. For example, the white diagonal

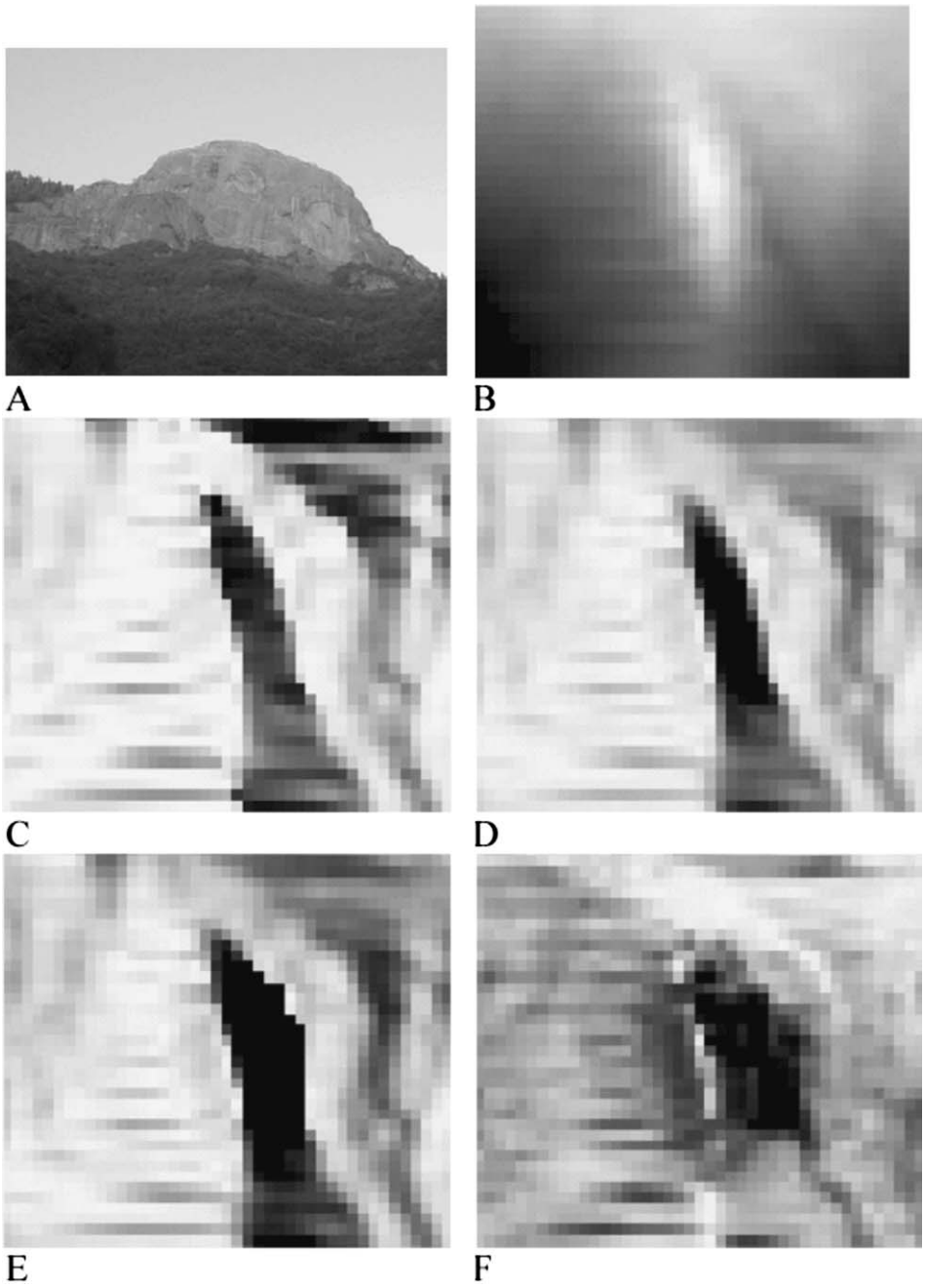

Figure 2. (A) Moro Rock is a large narrow granitic outcrop about 1.2 km long. The photo is from the west. The following maps are oriented towards the north. (B) DEM of the Moro Rock area is used to illustrate the differences between the radiation proxies draped over a drastic terrain feature (high elevations are lighter). (C) Transformed aspect map (high radiation areas are lighter). (D) Transformed aspect modified by slope. (E) Hillshade with $A = 225$, $S = 45$. (F) Potential relative radiation (PRR).

in the center of the image is the ridgeline of Moro Rock. Also, the flat area in the upper middle of the image is readily identifiable in Figure 2f. An artifact of these methods appears in Figure 2c-f where horizontal striping is present. DEMs can often have defects and these affect all spatial based radiation models. This can cause serious problems in low-re-

Table 1. Correlations between field- and DEM-derived proxies and PRR with the site-specific modeled radiation with FACET for 99 sample plots in Kaweah Basin, and with the Smith (2002) model for 175 sample plots in H.J. Andrews Experimental Forest. One-thousand randomly located points were also used to sample values from the Smith (2002) model and the digitally derived proxies for the H.J. Andrews Experimental Forest.

Radiation Proxy	Modeled Radiation		
	Facet (r^2)	Smith (r^2)	1000pts (r^2)
Transformed field aspect	0.05	0.06	
Transformed field aspect * sine slope	0.08	0.05	
Transformed DEM aspect	0.24	0.09	0.20
Transformed DEM aspect* sine DEM slope	0.30	0.05	0.14
Hillshade	0.28	0.31	0.20
PRR	0.81	0.54	0.59

lief terrain and probably weakened our results in Sequoia.

To quantify the amount of variation captured by the different DEM-based indices we compare them to the radiation Figures generated by the FACET model's radiation algorithm for the 99 Kaweah Basin field plots and the Smith (2002) model for the 175 plots scattered across the HJA watershed (Table 1). Many of the sites with the most negative transformed aspect have relatively high radiation according to the more sophisticated models. Adding the slope modification improves the correlation for the Kaweah data but actually decreases the explanatory power for the HJA data. However, both of these changes are small compared to the change derived from the PRR model below. Arc/Info's Hillshade function mirrors the assumptions from transformed aspect, adding the effects of shading by adjacent topography. The Hillshade proxy represents solar conditions at one point in time. Under these conditions, few of the 99 points in Kaweah Basin were topographically shaded, and the Hillshade index is roughly equivalent to the transformed aspect proxy. By contrast, topographic shading is much more important for the 175 points in HJA due to both topography and higher latitude.

The PRR proxy captures any potential shading that occurs throughout the course of the day and year. The index is highly correlated with radiation values obtained from the Smith and FACET models (Table 1). Correlations between PRR and the Facet model vary from month to month, with the lowest correlations occurring around the summer solstice (Table 2). After inspecting scatter plots from each month, we found the total variance in monthly radiation was much larger during the equinoxes due to larger zenith angles (Table 2). The FACET model does not account for topographic shading, an effect included in the PRR measure. By recalculating the index without including shadowing, we found that topographic shading accounted for most of the two to seven percent difference between our PRR proxy and the FACET-modeled radiation. Due to potential biases in the placement of the HJA field plots, correlations between the DEM-derived indices and the Smith model also were compared for 1000 points randomly sampled across the landscape (Table 1). Again, PRR is highly correlated with the modeled radiation. Transformed aspect does as well as Hillshade in predicting this larger dataset of radiation values.

Table 2. Correlations between potential relative radiation index and modeled radiation by month and cumulatively for 99 Kaweah Basin plots. Additionally, September was modeled without calculating shadows. This is the closest approximation to the calculations performed in the FACET radiation routine. The difference in correlation appears to be due to shading and the variation in radiation from month to month due to the solar zenith. Topographic effects account for more variation during the solstices when the zenith angle is larger. The variance column shows the proportion of the maximum described variation in PRR for each month.

Month	FACET (r^2)	Variance
March	0.86	1.00
April	0.82	0.58
May	0.76	0.25
June	0.63	0.16
July	0.68	0.21
August	0.83	0.46
September	0.94	0.82
Sum	0.90	
Sept w/no shad	0.98	

Field-derived measurements of transformed aspect and slope-modified transformed aspect correspond poorly with the modeled radiation and the other radiation proxies. They explain less than nine percent of the variation in FACET-modeled radiation values and less than seven percent of the variation from the

Smith model (Table 1). Correspondence between the field-based proxies and PRR are equally poor. These low correlations underscore that field measurements of many environmental variables, including slope and aspect, can be estimated for different scales than measurements derived from a 30-m DEM. This can cause the two approaches to differ substantially in their final estimates.

Discussion

Our calculation of potential relative radiation (PRR) accounts for both temporal variation and topographic shading by adjacent landforms and requires only digital elevation data and access to Arc/Info or similar GIS software. The method can be implemented for most study areas with only an afternoon's time investment on a reasonably fast computer (e.g., a large DEM with about 45 million grid cells, took about 8 hours). We feel the index provides a good compromise between the simplicity of common radiation proxies and the complexity of more sophisticated models. It captures the dynamics important to radiation in mountainous terrain, but remains accessible to a wide user group.

Studies that explicitly model radiation in topographically heterogeneous areas regularly find radiation effects to be important correlates with vegetation pattern (Davis and Goetz 1990; Franklin 1998). Studies based on proxies such as aspect tend to be more variable in their conclusions (Parker 1995; Guisan et al. 1998; Donegan and Rebertus 1999; Park 2001). Proxy variables continue to be used in vegetation analysis, however, because they are much easier to derive. We show that these proxies can correspond poorly with modeled radiation for sample sizes realistic of a rigorous field effort. Given enough samples, transformed aspect predicts radiation as well as Hillshade (Table 1). With smaller sample sizes, the differences might be considerable, particularly if many of the samples are in topographic shade as was the case for the 175 sample plots considered in this study (Table 1).

The PRR index, which also can be calculated easily from digital terrain data, provides a much better match to the modeled radiation for the field locations. Much of this increased correlation can be explained by two factors. First, the ability to account for topographic shading captures the topographic context. Shadows from adjacent ridges produce areas that are considerably darker during certain hours of the day, and nonspatial models, that do not incorporate local topography, can greatly overestimate radiation at these sites. Second, temporal integration captures the dynamic aspect of solar geometry which is absent in static proxies.

PRR has been used in several studies and been shown to improve upon more conventional measures of slope and aspect at estimating spatial patterns of temperature (Lookingbill and Urban 2003), soil moisture (Lookingbill and Urban 2004), and tree growth (Bunn et al. 2003). PRR also is being used in regional vegetation mapping projects in Washington and Oregon and has had greater explanatory power than other simpler radiation proxies (unpublished data).

It is important to reiterate that our method provides relative estimates only. We modeled the most predictable source of heterogeneity, direct-beam radiation with clear-sky conditions and no diffuse-beam radiation. While this is not completely realistic, it approximates the most common growing season condition in the mountainous western US systems in which we work. We present our proxy as an upper bound of potential radiation differences. Radiation from diffuse sources tends to attenuate the overall variability caused by topography, as overcast skies cast a reasonably uniform light across the entire landscape (Dubayah and Rich 1995).

Finally, because our method is so reliant on DEM data, any inherent errors in the DEMs will propagate into the results. We did not employ DEM-correction algorithms as they sometimes introduce as many errors as they remove (Dubayah 1994; Dubayah and Rich 1995) and we wanted to keep our method as simple as possible. We advise that all DEMs be examined for apparent systematic errors and stress the importance of obtaining the best terrain data possible.

Conclusion

Radiation is a fundamental influence on many ecological patterns. We developed our approach for use in forest community studies to respond to the following common data needs: (1) Our study areas encompass large landscapes in mountainous terrain, in which empirical measures of radiation are sparsely available; (2) In the complex terrain in which we work, we felt differences associated with topographic shading were important to include in our estimates of

radiation. We also felt that it was important to represent the dynamic nature of radiation loads, which change over the course of the day and year; (3) Because our requirements for vegetation analysis are less stringent then for atmospheric scientists, we did not account for the comprehensive suite of factors used in solar radiation models such as attenuation by atmospheric transmittance or cloudiness. This is in part because of the scale of our study, and also because our analyses of vegetation distributions are correlative and thus require only relative radiation values. We felt it was important that the estimates could be calculated readily and the approach be widely accessible. The resulting PRR index should provide a tool for estimating fine-scale variability in radiation across large spatial extents.

Acknowledgements

We thank Peter Harrell and Andy Bunn for their assistance and comments on this project. This research was supported in part by a USGS/BRD Coop. Agreement No. 99WRAG0019 and partially by NSF grant IBN-9652656 to D.L. Urban.

References

Austin M.P., Nicholls A.O. and Margules C.R. 1990. Measurement of the Realized Qualitative Niche: Environmental Niches of Five Eucalyptus Species. Ecological Monographs 60(2): 161–177.

Band L.E., Peterson D.L., Running S.W., Coughlan J., Lammers R., Dungan J. and Nemani R. 1991. Forest ecosystem process at the watershed scale: basis for distributed simulation. Ecological Modelling 56: 171–196.

Beers T.W., Press P.E. and Wensel L.C. 1966. Aspect transformation in site productivity research. Journal of Forestry 64: 691–692.

Bolstad P., Swank W. and Vose J. 1998. Predicting southern Appalachian overstory vegetation with digital terrain data. Landscape Ecology 13: 695–707.

Bonan G.B. 1988. Environmental processes and vegetation patterns in boreal forests. Ph.D. Thesis, University of Virginia, Charlottesville, Virginia, USA.

Brown D.G. 1994. Predicting vegetation types at treeline using topography and biophysical disturbance variables. Journal of Vegetation Science 5: 641–656.

Bunn A.G., Lawrence R.L., Bellante G.J., Waggoner L.A. and Graumlich L.J. 2003. Spatial variation in distribution and growth patterns of old growth strip-bark pines. Arctic, Antarctic and Alpine Research 35: 323–330.

Callaway R.M., Clebsch E.E.C. and White P.S. 1998. A Multivariate analysis of forest communities in the western Great Smoky Mountains national park. American Midland Naturalist 118: 107–118.

Campbell G.S. and Norman J.M. 1998. An Introduction to Environmental Biophysics. Springer, New Jersey, USA.

Chen J., Saunders S.C., Crow T.R., Naiman R.J., Brosofske K.D., Mroz G.D., Brookshire B.L. and Franklin J.F. 1999. Microclimate in forest ecosystem and landscape ecology. Bioscience 49: 288–97.

Clinton B.D., Boring L.R. and Swank W.T. 1994. Regeneration patterns in canopy gaps of mixed-oak forests of the Southern Appalachians: Influences of topographic position and evergreen understory. American Midland Naturalist 132: 308–319.

Daly C., Neilson R.P. and Phillips D.L. 1994. A statistical-topographic model for mapping climatological precipitation over mountainous terrain. Journal of Applied Meteorology 33: 140–158.

Davis. F.W. and Goetz S. 1990. Modeling vegetation pattern using digital terrain data. Landscape Ecology 4: 69–80.

Day F.P. and Monk C.D. 1974. Vegetation patterns on a southern Appalachian watershed. Ecology 55: 1064–1074.

Donnegan. J.A. and Rebertus A.J. 1999. Rates and mechanisms of subalpine forest succession along an environmental gradient. Ecology 80: 1370–1384.

Dozier J. and Frew J. 1990. Rapid calculation of terrain parameters for radiation modeling from digital elevation data. IEEE Transaction on Geoscience and Remote Sensing 28: 963–969.

Dubayah R.C. 1994. Modeling a solar radiation topoclimatology for the Rio Grande River Basin. Journal of Vegetation Science 5: 627–640.

Dubayah R. and Rich P.M. 1995. Topographic solar radiation models in GIS. International Journal of Geographical Information Systems 9: 405–419.

Dyrness C.T., Franklin J.F. and Moir W.H. 1974. A preliminary classification of forest communities in the central portion of the Western Cascades in Oregon. Forestry Sciences Laboratory, USDA Forest Service, Corvallis, OR, USA.

ESRI, ARC/Info 7. 1994. Environmental Systems. Research Institute Inc, Redlands, CA, USA.

Frank E.C. and Lee R. 1966. Potential solar beam irradiation on slopes: tables for 30 to 50 latitude. Rocky Mountain For. Range Exp. Stn. Gen. Tech. Rep. U.S.D.A Forest Service.

Franklin J. 1998. Predicting the distribution of shrub species in southern California from climate and terrain-derived variables. Journal of Vegetation Science 9: 733–748.

Franklin J.F. and C.T. Dyrness. 1988. Natural vegetation of Oregon and Washington. Oregon State University Press, Corvallis, OR, USA.

Franklin J., McCullough P. and Gray C. 2000. Terrain variables used for predictive mapping of vegetation communities in Southern California.. In: Wilson J.P. and Gallant J.C. (eds), Terrain Analysis: Principle and Applications. John Wiley and Sons, New York, USA, pp. 331–354.

Fu P. and Rich P.M. 1999. Design and implementation of the Solar Analyst: an ArcView extension for modeling solar radiation at landscape scales. Proceedings of the 19th Annual ESRI User Conference, San Diego, USA. Available from http://www.esri-.com/library/userconf/proc99/proceed/papers/pap867/p867.htm.

Geiger R.J. 1965. The Climate Near the Ground. Harvard University Press, Cambridge, MA, USA.

Greenland D. 1996. Potential solar radiation at the H. J. Andrews experimental forest. Pacific Northwest Research Station, U.S.D.A. Forest Service.

Grier C.C. and Logan R.S. 1977. Old-growth *Pseudotsuga menziesi* communities of a western Oregon watershed: biomass distribution and production budgets. Ecological Monographs 47: 373–400.

Guisan A., Theurillat J. and Kienast F. 1998. Predicting the potential distribution of plant species in an alpine environment. Journal of Vegetation Science 9: 65–74.

Kessell S.R. 1979. Gradient Modeling: Resource and Fire Management. Springer-Verlag, New York, USA.

Klein S.A. 1977. Calculation of monthly average insolation on tilted surfaces. Solar Energy 19: 325–329.

Lookingbill T. and Urban D. 2003. Spatial estimation of air temperature differences for landscape-scale studies in montane environments. Agricultural and Forest Meteorology 114: 141–151.

Lookingbill T. and Urban D. 2004. An empirical approach towards improved spatial estimates of soil moisture for vegetation analysis. Landscape Ecology 19: 417–433.

Mackey B.G., Mullen I.C., Baldwin K.A., Gallant J.C., Sims R.A. and McKenney D.W. 2000. Towards a spatial model of boreal forest ecosystems: The role of digital terrain analysis.. In: Wilson J.P and Gallant J.C. (eds), Terrain Analysis: Principle and Applications. John Wiley and Sons, New York, USA, pp. 391–427.

McCay D.H., Abrams M.D. and DeMeo T.E. 1997. Gradient analysis of secondary forests of eastern West Virginia. Journal of the Torrey Botanical Society 124: 160–173.

McKenney D.W., Mackey B.G. and Zavitz B.L. 1999. Calibration and sensitivity analysis of a spatially-distributed solar radiation model. Int. J. Geographical Information Science 13: 49–65.

Miller C. and Urban D.L. 1999. A model of surface fire, climate and forest pattern in the Sierra Nevada, California. Ecological Modelling 114: 113–135.

Nikolov N.T. and Zeller K.F. 1992. A solar radiation algorithm for ecosystem dynamic models. Ecological Modelling 61: 149–168.

Park A.D. 2001. Environmental influences on post-harvest natural regeneration in mexican pine-oak forests. Forest Ecology and Management 144: 213–228.

Parker A.J. 1995. Comparative gradient structure and forest cover types in Lassen Volcanic and Yosemite National Parks, California. Bulletin of the Torrey Botanical Society 122: 58–68.

Raven P.H., Evert R.F. and Eichhorn S.E. 1992. Biology of Plants. Worth Publishers, New York, USA.

Running S.W., Nemani R.R. and Hungerford R.D. 1987. Extrapolation of synoptic meteorological data in mountainous terrain and its use for simulating forest evapotranspiration and photosynthesis. Canadian Journal of Forest Research 17: 472–483.

Smith J. 2002. Mapping the Thermal Climate of the H. J. Andrews Experimental Forest, Oregon. M.S. Thesis, Oregon State University, Corvallis, OR, USA.

Stephenson N.L. 1998. Actual evapotranspiration and deficit: biologically meaningful correlates of vegetation distribution across spatial scales. Journal of Biogeography 25: 855–870.

Stephenson N.L. and Parsons D.J. 1993. A research program for predicting the effects of climate change on the Sierra Nevada.. In: Viers S.D. Jr., Stohlgren T.J. and Schonewal-Cox C. (eds), Proceedings of the Fourth Conference on Research in California's National Parks. USDI Park Service Transactions and Proceedings Series 9, pp. 93–109.

Swanson F.J., Kratz T.K., Caine N. and Woodmansee R.G. 1988. Landform effects on ecosystem patterns and processes. Bioscience 38: 92–98.

Thornton P.E., Running S.W. and White M.A. 1997. Generating surfaces of daily meteorological variables over large regions of complex terrain. Journal of Hydrology 190: 214–251.

Urban D.L., Miller C., Halpin P.N. and Stephenson N.L. 2000. Forest gradient response in Sierran landscapes: the physical template. Landscape Ecology 15: 603–620.

Vankat J.L. and Major J. 1978. Vegetation changes in Sequoia National Park, California. Journal of Biogeography 5: 377–402.

Wilson J.P. and Gallant J.C. 2000. Secondary topographic attributes.. In: Wilson J.P. and Gallant J.C. (eds), Terrain Analysis: Principle and Applications. John Wiley and Sons, New York, USA, pp. 97–132.

Whittaker R.H. 1956. Vegetation of the Great Smoky Mountains. Ecological Monographs. 26: 1–80.

Whittaker R.H. 1960. Vegetation of the Siskiyou Mountains, Oregon and California. Ecological Monographs 30: 279–338.

Yeakley J.A., Swank W.T., Swift L.W., Hornberger G.M. and Shugart H.H. 1998. Soil moisture gradients and controls on a southern Appalachian hillslope from drought through recharge. Hydrology and Earth System Sciences 2: 41–49.